Energy dissipative numerical schemes for gradient flows of planar curves

Tomoya Kemmochi

Department of Applied Physics, Graduate School of Engineering,
Nagoya University

1. Introduction

In this study, we develop numerical methods for the L^2-gradient flow of a planar curve of the form

$$\mathbf{u}_t = -\operatorname{grad} E(\mathbf{u}), \quad t > 0, \tag{1}$$

where $\mathbf{u}$ is a time-dependent closed planar curve, E is a given energy functional, and $\operatorname{grad} E$ is the Fréchet derivative with respect to the L^2-structure with line integral ds. The gradient flow (1) is energy dissipative since

$$\frac{d}{dt}E[\mathbf{u}] = -\int |\operatorname{grad} E(\mathbf{u})|^2 ds \leq 0.$$

Typical examples are the curve shortening flow (the curvature flow)

$$\mathbf{u}_t = \boldsymbol{\kappa} \tag{2}$$

and the elastic flow (the Willmore flow)

$$\mathbf{u}_t = -2\varepsilon^2\left(\nabla_s^2\boldsymbol{\kappa} + \frac{1}{2}|\boldsymbol{\kappa}|^2\boldsymbol{\kappa}\right) + \boldsymbol{\kappa} \tag{3}$$

with energy functionals

$$E[\mathbf{u}] = \int ds, \quad \text{and} \quad E[\mathbf{u}] = \varepsilon^2\int |\boldsymbol{\kappa}|^2 ds + \int ds,$$

respectively, where $\boldsymbol{\kappa} = -\mathbf{u}_{ss}$ is the curvature vector and ∇_s is the normal component of the arc-length derivative ∂_s. Note that the elastic flow is a fourth-order nonlinear evolution equation.

The purpose of this study is to construct a dissipative numerical scheme for (1), i.e., a scheme which has the discrete energy dissipation property $E[\mathbf{u}_h^{n+1}] \leq E[\mathbf{u}_h^n]$ at each time step. In general, a numerical method that retains a certain property for a target equation is called structure-preserving. It is known that the numerical solutions obtained by these methods are not only physically realistic but also have the advantage of numerical stability (cf. [3, 4]). In particular, structure-preserving methods are suitable for computations over long time intervals.

In [5], we proposed a novel framework to construct structure-preserving numerical schemes for (1). We introduce our results in the present article. Our method is based on the discrete partial derivative method (DPDM) [7], which is a framework to construct structure-preserving schemes for dissipative and conservative problems. We extend the strategy of DPDM and derive a temporally discrete scheme for (1). The principal idea is to discretize the chain rule rather than the equation (1) itself.

Our temporally discrete scheme can be formulated as a weak form. Therefore, for the elastic flow (3), the scheme requires both trial and test functions to be twice differentiable. In order to ensure the differentiability in the Galerkin method, we discretize curves by B-splines [11], which are piecewise polynomials and continuously differentiable. When we use piecewise polynomials of degree p, corresponding B-splines are C^{p-1}-functions. Thus we can derive a fully discretized scheme for the elastic flow (3) with B-splines of degree $p \geq 3$.

Further, we will present a new result that was obtained *after* the conference. We consider the area preserving curve shortening flow

$$\mathbf{u}_t = \boldsymbol{\kappa} - \langle \boldsymbol{\kappa} \rangle, \tag{4}$$

where

$$\langle \boldsymbol{\kappa} \rangle = L[\mathbf{u}]^{-1} \int \boldsymbol{\kappa} \cdot \boldsymbol{\nu} ds \boldsymbol{\nu}, \quad L[\mathbf{u}] = \int ds,$$

and $\boldsymbol{\nu}$ is the outward normal vector of the curve $\mathbf{u}$. This equation has both the energy (length) dissipation and the area preservation:

$$\frac{d}{dt} L[\mathbf{u}] \leq 0, \quad \frac{d}{dt} A[\mathbf{u}] = 0,$$

where $A[\mathbf{u}]$ is the area of the domain enclosed by the curve $\mathbf{u}$. We will give a numerical scheme that inherits these two properties according to the idea of [8].

The rest of this article is organized as follows. In Section 2, we will introduce DPDM for gradient flows of graphs of functions in order to explain the strategy to construct structure-preserving numerical schemes. Section 3 is devoted to present our temporal approximation scheme for gradient flows (1) that preserves the energy dissipation, and we give fully discrete scheme in Section 4 with a short introduction to B-spline curves. In Section 5, we present examples of the discrete gradient for the curve shortening flow (2) and the elastic flow (3), which play an important roles in our scheme. In Section 6, the area preserving curve shortening flow is considered and we construct a numerical scheme that preserves the length dissipation and the area preservation. We present numerical examples in Section 7, and finally concluding remarks are given in Section 8.

2. Discrete partial derivative method

In order to present the strategy to construct numerical schemes that preserves the energy dissipation, we introduce the *discrete partial derivative method* (DPDM) for L^2-gradient flows of graphs of functions. The topic of this section is based on [7].

In this section, we consider an L^2-gradient flow of the form

$$u_t = -\frac{\delta E}{\delta u}, \quad t > 0, \tag{5}$$

where $\frac{\delta E}{\delta u}$ is the first variation of a given energy functional E. Owing to the chain rule, one can easily see that the flow (5) has dissipation property as follows:

$$\frac{d}{dt} E[u] = \int_\Omega \frac{\delta E}{\delta u} u_t \, dx = - \int_\Omega |u_t|^2 dx \leq 0, \tag{6}$$

where Ω is the domain in which equation (5) is considered.

We observe the above procedure in more detail. Although we can consider general energy functional, we assume that E is represented as

$$E[u] = \int_0^1 G(u, u_x) dx$$

for functions u defined over an interval $I = (0, 1)$, where $G = G(u, p)$ is a given density function. Then, we have

$$\begin{aligned}
\frac{d}{dt}E[u] &= \int_I \frac{\partial}{\partial t} G(u, u_x) dx \\
&= \int_I [G_u(u, u_x)u_t + G_p(u, u_x)u_{xt}] dx \\
&= \int_I \left[G_u(u, u_x) - \frac{\partial}{\partial x} G_p(u, u_x) \right] u_t \, dx \\
&= \int_I \frac{\delta E}{\delta u} u_t \, dx,
\end{aligned}$$

under an appropriate boundary condition such as the periodic boundary condition. Therefore, we can obtain the energy dissipation (6) from the chain rule for the density function

$$\frac{\partial}{\partial t} G(u, u_x) = G_u(u, u_x)u_t + G_p(u, u_x)u_{xt} \tag{7}$$

and the integration by parts.

Now, we introduce DPDM, which is a time-discretization method for gradient flows of the form (5). The key strategy of this method is to discretize the chain rule (7). We first discretize the differentiation in time by difference quotients. Let t_n be a discrete time level and u^n be the corresponding discrete solution. We replace the left-hand-side of (7) and u_t by

$$\frac{G(u^{n+1}, u_x^{n+1}) - G(u^n, u_x^n)}{\tau_n} \qquad \text{and} \qquad \frac{u^{n+1} - u^n}{\tau_n},$$

respectively, where $\tau_n := t_{n+1} - t_n = \tau_n$. Then, we may get the following equation:

$$\frac{G(u^{n+1}, u_x^{n+1}) - G(u^n, u_x^n)}{\tau_n} = A \frac{u^{n+1} - u^n}{\tau_n} + B \frac{u_x^{n+1} - u_x^n}{\tau_n}$$

for appropriate functions A and B. If we can find such functions, we define the discrete first variation by

$$\frac{\delta E_{\mathrm{d}}}{\delta(u^{n+1}, u^n)} := A - \frac{\partial}{\partial x} B$$

and the discrete gradient flow by

$$\frac{u^{n+1} - u^n}{\tau_n} = -\frac{\delta E_{\mathrm{d}}}{\delta(u^{n+1}, u^n)}. \tag{8}$$

Then, we have, under an appropriate boundary condition,

$$\frac{E[u^{n+1}] - E[u^n]}{\tau_n} = \int_I \left(A \frac{u^{n+1} - u^n}{\tau_n} + B \frac{u_x^{n+1} - u_x^n}{\tau_n} \right) dx$$

$$
\begin{aligned}
&= \int_I \left(A - \frac{\partial}{\partial x} B \right) \frac{u^{n+1} - u^n}{\tau_n} dx \\
&= \int_I \frac{\delta E_\mathrm{d}}{\delta(u^{n+1}, u^n)} \frac{u^{n+1} - u^n}{\tau_n} dx \\
&= - \int_I \left| \frac{u^{n+1} - u^n}{\tau_n} \right|^2 dx \\
&\leq 0,
\end{aligned}
$$

which shows that the discrete equation (8) preserves the energy dissipation.

Since A and B correspond to the partial derivatives G_u and G_p respectively, these functions are called discrete partial derivatives and denoted by

$$
A = \frac{\partial G_\mathrm{d}}{\partial(u^{n+1}, u^n)}, \quad B = \frac{\partial G_\mathrm{d}}{\partial(u_x^{n+1}, u_x^n)}.
$$

Although they are not unique in general, we use these symbols to describe one of them. We can construct discrete partial derivatives for a lot of energy density functions appearing in applications. Let us consider the Allen-Cahn equation as an example. In this case, the energy density function is described by

$$
G(u, p) = \frac{1}{2}|p|^2 + \frac{1}{4\varepsilon^2}(u^2 - 1)^2
$$

for a positive parameter ε. Then, we have

$$
G(u, u_x) - G(v, v_x) = \frac{u_x + v_x}{2}(u_x - v_x) + \frac{(u^2 + v^2 - 2)(u + v)}{4\varepsilon^2}(u - v),
$$

which means

$$
\frac{\partial G_\mathrm{d}}{\partial(u^{n+1}, u^n)} = \frac{(u^2 + v^2 - 2)(u + v)}{4\varepsilon^2}, \quad \frac{\partial G_\mathrm{d}}{\partial(u_x^{n+1}, u_x^n)} = \frac{u_x + v_x}{2}.
$$

Therefore, the scheme of the DPDM for the Allen-Cahn equation is

$$
\frac{u^{n+1} - u^n}{\tau_n} = \frac{u_{xx} + v_{xx}}{2} - \frac{(u^2 + v^2 - 2)(u + v)}{4\varepsilon^2}.
$$

If we impose the homogeneous Neumann boundary condition, we can obtain the discrete energy dissipation. Generally, if the density function G is given by

$$
G(u, p) = \sum_{m=1}^{M} f_m(u) g_m(p)
$$

for some functions f_m and g_m, then we can construct the discrete partial derivatives by

$$
\begin{aligned}
\frac{\partial G_\mathrm{d}}{\partial(u, v)} &= \sum_{m=1}^{M} \frac{f_m(u) - f_m(v)}{u - v} \frac{g_m(u_x) + g_m(v_x)}{2}, \\
\frac{\partial G_\mathrm{d}}{\partial(u_x, v_x)} &= \sum_{m=1}^{M} \frac{f_m(u) + f_m(v)}{2} \frac{g_m(u_x) - g_m(v_x)}{u_x - v_x},
\end{aligned}
$$

where we recognize that $(f_m(u)-f_m(v))/(u-v) = f'_m(u)$ and $(g_m(u_x)-g_m(v_x))/(u_x-v_x) = g'_m(u_x)$ when $u = v$.

We mention the space discretization of (8). Recalling that (8) is equivalent to

$$\frac{u^{n+1}-u^n}{\tau_n} = -\frac{\partial G_{\mathrm{d}}}{\partial(u^{n+1},u^n)} + \frac{\partial}{\partial x}\frac{\partial G_{\mathrm{d}}}{\partial(u_x^{n+1},u_x^n)},$$

we can derive the weak formulation

$$\left(\frac{u^{n+1}-u^n}{\tau_n}, v\right)_I = -\left(\frac{\partial G_{\mathrm{d}}}{\partial(u^{n+1},u^n)}, v\right)_I - \left(\frac{\partial G_{\mathrm{d}}}{\partial(u_x^{n+1},u_x^n)}, v_x\right)_I, \qquad \forall v,$$

under appropriate boundary condition, where $(u,v)_I = \int_I uv dx$. Therefore, we can discretize the above equation by the Galerkin method, and we obtain the fully discrete scheme of (5). Moreover, the energy dissipation property is preserved even in this case. Indeed, substituting $v = (u^{n+1}-u^n)/\tau_n$ as a test function, then we obtain

$$\frac{E[u^{n+1}]-E[u^n]}{\tau_n} = -\int_I \left|\frac{u^{n+1}-u^n}{\tau_n}\right|^2 dx \le 0,$$

which is valid even for the Galerkin method.

3. Structure-preserving temporal discretization for gradient flows of planar curves

Now, we consider gradient flows of the form (1) for planar curves. In this case, we discretize the chain rule

$$\frac{d}{dt}E[\mathbf{u}] = \int \operatorname{grad} E(\mathbf{u}) \cdot \mathbf{u}_t \, ds(\mathbf{u}),$$

for the energy functional E, rather than the density function, where we write $ds(\mathbf{u})$ to emphasize the dependence of the line element.

As in the previous section, we first replace the time derivatives $\frac{d}{dt}E[\mathbf{u}]$ and $\mathbf{u}_t$ by the differences $E[\mathbf{u}] - E[\mathbf{v}]$ and $\mathbf{u} - \mathbf{v}$, respectively, for curves $\mathbf{u}$ and $\mathbf{v}$. In contrast to the graph case, however, we should also replace the line element $ds(\mathbf{u})$ by appropriate measure. Although there may be several choices, e.g., $ds(\mathbf{u})$, $ds(\mathbf{v})$, and $ds((\mathbf{u}+\mathbf{v})/2)$, we here choose $ds((\mathbf{u}+\mathbf{v})/2)$. This choice will be validated in a sense when considering the area preserving curve shortening flow (Section 6). Then, we define the discrete gradient $\operatorname{grad}_{\mathrm{d}} E$ as follows.

Definition 3.1 (Discrete gradient). The discrete gradient $\operatorname{grad}_{\mathrm{d}} E$ is defined as the function that satisfies the relation

$$E[\mathbf{u}] - E[\mathbf{v}] = \int \operatorname{grad}_{\mathrm{d}} E(\mathbf{u},\mathbf{v}) \cdot (\mathbf{u}-\mathbf{v}) \, ds\left(\frac{\mathbf{u}+\mathbf{v}}{2}\right) \tag{9}$$

for any curves $\mathbf{u}$ and $\mathbf{v}$.

If we can find such $\operatorname{grad_d} E$, the temporally discretized scheme is constructed by

$$\frac{\mathbf{u}^{n+1}-\mathbf{u}^n}{\tau_n} = -\operatorname{grad_d} E(\mathbf{u}^{n+1}, \mathbf{u}^n),$$

where τ_n is the time increment and $\mathbf{u}^n$ denotes the approximated solution at the n-th step. Then, by the definition (9), the discrete energy dissipation $E[\mathbf{u}^{n+1}] \le E[\mathbf{u}^n]$ is clearly established.

We present how to construct such discrete gradients. In order to describe that, we set $I=(0,1)$ and

$$\mathbf{H}^m_\pi = \{\mathbf{v} \in H^m(I)^2 \mid \mathbf{v}^{(i)}(0) = \mathbf{v}^{(i)}(1),\ i=0,1,\ldots,m-1\},$$

which is the space of closed curves of class H^m for $m \ge 1$. We denote the variable of the parameter of curves by z. Now, assume that the energy E is given in the form

$$E[\mathbf{u}] = \int F(\mathbf{u}_z, \mathbf{u}_{zz}) ds, \quad \mathbf{u} \in \mathbf{H}^2_\pi.$$

Then, with the line element $|\mathbf{u}_z|$, we can write

$$E[\mathbf{u}] = \int_0^1 F(\mathbf{u}_z, \mathbf{u}_{zz}) |\mathbf{u}_z| dz.$$

Thus, letting $G(\mathbf{u}_z, \mathbf{u}_{zz}) := F(\mathbf{u}_z, \mathbf{u}_{zz})|\mathbf{u}_z|$, we can consider discrete partial derivatives of the new density function G, and we have

$$E[\mathbf{u}] - E[\mathbf{v}] = \int_0^1 \left[\frac{\partial G_d}{\partial(\mathbf{u}_z, \mathbf{v}_z)} \cdot (\mathbf{u}_z - \mathbf{v}_z) + \frac{\partial G_d}{\partial(\mathbf{u}_{zz}, \mathbf{v}_{zz})} \cdot (\mathbf{u}_{zz} - \mathbf{v}_{zz}) \right] dz. \tag{10}$$

Here, $\frac{\partial G_d}{\partial(\mathbf{u}_z, \mathbf{v}_z)}$ is a vector-valued discrete partial derivative of the form

$$\frac{\partial G_d}{\partial(\mathbf{u}_z, \mathbf{v}_z)} = \left(\frac{\partial G_d}{\partial(u_{1,z}, v_{1,z})}, \frac{\partial G_d}{\partial(u_{2,z}, v_{2,z})} \right)^T,$$

where $\mathbf{u} = (u_1, u_2)$ and $\mathbf{v} = (v_1, v_2)$. The function $\frac{\partial G_d}{\partial(\mathbf{u}_{zz}, \mathbf{v}_{zz})}$ is defined in the same fashion. Therefore, integrating by parts, we have

$$\begin{aligned} E[\mathbf{u}] - E[\mathbf{v}] &= \int_0^1 \left[-\frac{\partial}{\partial z} \frac{\partial G_d}{\partial(\mathbf{u}_z, \mathbf{v}_z)} + \frac{\partial^2}{\partial z^2} \frac{\partial G_d}{\partial(\mathbf{u}_{zz}, \mathbf{v}_{zz})} \right] \cdot (\mathbf{u} - \mathbf{v}) dz \\ &= \int \left| \frac{\mathbf{u}_z + \mathbf{v}_z}{2} \right|^{-1} \left[-\frac{\partial}{\partial z} \frac{\partial G_d}{\partial(\mathbf{u}_z, \mathbf{v}_z)} + \frac{\partial^2}{\partial z^2} \frac{\partial G_d}{\partial(\mathbf{u}_{zz}, \mathbf{v}_{zz})} \right] \cdot (\mathbf{u} - \mathbf{v}) ds \Big(\frac{\mathbf{u} + \mathbf{v}}{2} \Big) \end{aligned}$$

for $\mathbf{u}, \mathbf{v} \in \mathbf{H}^4_\pi$, which allows us to define

$$\operatorname{grad_d} E(\mathbf{u}, \mathbf{v}) = \left| \frac{\mathbf{u}_z + \mathbf{v}_z}{2} \right|^{-1} \left[-\frac{\partial}{\partial z} \frac{\partial G_d}{\partial(\mathbf{u}_z, \mathbf{v}_z)} + \frac{\partial^2}{\partial z^2} \frac{\partial G_d}{\partial(\mathbf{u}_{zz}, \mathbf{v}_{zz})} \right].$$

We notice that the discrete gradient $\operatorname{grad_d} E$ is not unique as in the case for discrete partial derivatives.

From the above construction, the discrete gradient flow is described as

$$\frac{\mathbf{u}^{n+1}-\mathbf{u}^n}{\tau_n} = -\left|\frac{\mathbf{u}_z^{n+1}+\mathbf{u}_z^n}{2}\right|^{-1}\left[-\frac{\partial}{\partial z}\frac{\partial G_d}{\partial(\mathbf{u}_z^{n+1},\mathbf{u}_z^n)} + \frac{\partial^2}{\partial z^2}\frac{\partial G_d}{\partial(\mathbf{u}_{zz}^{n+1},\mathbf{u}_{zz}^n)}\right]. \tag{11}$$

Moreover, we can derive the weak formulation of the scheme. Multiplying (11) by arbitrary $\mathbf{v}\in\mathbf{H}^2_\pi$ and integrating over the curve $(\mathbf{u}^{n+1}+\mathbf{u}^n)/2$, we have

$$\begin{aligned}&\left(\left|\frac{\mathbf{u}_z^{n+1}+\mathbf{u}_z^n}{2}\right|\frac{\mathbf{u}^{n+1}-\mathbf{u}^n}{\tau_n},\mathbf{v}\right)_I\\ &\qquad = -\left(\frac{\partial G_d}{\partial(\mathbf{u}_z^{n+1},\mathbf{u}_z^n)},\mathbf{v}_z\right)_I - \left(\frac{\partial G_d}{\partial(\mathbf{u}_{zz}^{n+1},\mathbf{u}_{zz}^n)},\mathbf{v}_{zz}\right)_I, \qquad \forall\mathbf{v}\in\mathbf{H}^2_\pi.\end{aligned} \tag{12}$$

We can also derive the energy dissipation from the weak formulation (12). Indeed, letting $\mathbf{v}=(\mathbf{u}^{n+1}-\mathbf{u}^n)/\tau_n$, we have

$$\int_0^1\left|\frac{\mathbf{u}^{n+1}-\mathbf{u}^n}{\tau_n}\right|^2\left|\frac{\mathbf{u}_z^{n+1}+\mathbf{u}_z^n}{2}\right|dz = -\frac{E[\mathbf{u}^{n+1}]-E[\mathbf{u}^n]}{\tau_n}$$

from the discrete chain rule (10). As in the graph case, this procedure is valid even in the Galerkin method.

4. Galerkin approximation by B-spline curves

In order to approximate the weak formulation (12) by the Galerkin method, we need finite dimensional subspace of $\mathbf{H}^2_\pi$. In this study, we use the space of B-spline curves, which is the space of continuously differentiable piecewise polynomials. Here, we introduce periodic B-splines and then present the fully-discretized scheme for (1).

We first introduce B-splines. We say that a set of points $\Xi=\{\xi_1,\xi_2,\dots,\xi_n\}\subset\mathbb{R}$ is a *knot vector* if $\xi_i\le\xi_{i+1}$ for all i.

Definition 4.1 (B-spline basis functions and B-spline curves)**.** Let $p\in\mathbb{N}=\{0,1,2,\dots\}$, $n\in\mathbb{N}_+=\mathbb{N}\setminus\{0\}$, and $\Xi=\{\xi_1,\xi_2,\dots,\xi_n\}$ be a knot vector.

(i) The *i-th B-spline basis function of degree p* with respect to Ξ is a piecewise polynomial function $N^\Xi_{p,i}$ that is generated by the following formula:

$$N^\Xi_{0,i}(\xi)=\chi_{[\xi_i,\xi_{i+1})}(\xi), \quad \xi\in\mathbb{R},$$

for $i=1,2,\dots,n-1$, and

$$N^\Xi_{p,i}(\xi)=\frac{\xi-\xi_i}{\xi_{i+p}-\xi_i}N^\Xi_{p-1,i}(\xi)+\frac{\xi_{i+p+1}-\xi}{\xi_{i+p+1}-\xi_{i+1}}N^\Xi_{p-1,i+1}(\xi), \quad \xi\in\mathbb{R},$$

for $i=1,2,\dots,n-p-1$ and $p\ge1$, where χ_J is the characteristic function of $J\subset\mathbb{R}$. Here, if $\xi_{i+p}=\xi_i$ (resp. $\xi_{i+p+1}=\xi_{i+1}$), then the term $(\xi-\xi_i)/(\xi_{i+p}-\xi_i)$ (resp. $(\xi_{i+p+1}-\xi)/(\xi_{i+p+1}-\xi_{i+1})$) is regarded as null.

(ii) A curve $\mathbf{u}\colon [a,b] \to \mathbb{R}^2$ is a *B-spline curve of degree p* if $\mathbf{u}$ is represented by

$$\mathbf{u}(z) = \sum_{i=1}^{n-p-1} N_{p,i}^{\Xi}(z)\mathbf{P}_i, \quad z \in [a,b],$$

for some knot vector Ξ and $n \in \mathbb{N}_+$. The coefficient $\mathbf{P}_i$ is called a *control point.*

In fact, if the knot vector is disjoint (i.e., $i \neq j \implies \xi_i \neq \xi_j$), then it is known that $N_{p,i}^{\Xi}$ is a C^{p-1}-function. For more details on the properties of B-spline functions, we refer the reader to [2, 9, 11].

In the present article, we only consider the periodic B-spline functions and curves. Let $I = [0,1]$, $p \in \mathbb{N}$, $N \in \mathbb{N}_+$, and $h = 1/N$. We define a knot vector Ξ by

$$\Xi = \{\xi_i\}_{i=1}^{N+2p+1} = \{-ph, -(p-1)h, \dots, 1+(p-1)h, 1+ph\}, \tag{13}$$

and let $N_{p,i} = N_{p,i}^{\Xi}$ be the corresponding B-spline basis function. In this case, if $N > p$, we can see that

$$\left(\frac{d}{dz}\right)^m N_{p,i}(0) = \left(\frac{d}{dz}\right)^m N_{p,i+N}(1),$$

for $i = 1, 2, \dots, p$ and $m = 0, 1, \dots, p-1$. Therefore, the function

$$B_{p,i}(z) = B_{h,p,i}(z) = \begin{cases} N_{p,i}(z), & z \in [0, \xi_{i+p+1}], \\ N_{p,i+N}(z), & z \in [\xi_{i+N}, 1], \\ 0, & \text{otherwise} \end{cases} \tag{14}$$

for each $i = 1, 2, \dots, p$ is a periodic C^{p-1}-function on I. The restriction $N_{p,i}|_I$ for $i > p$ is also C^{p-1}-periodic on I. Thus, we can define a closed B-spline curve as follows.

Definition 4.2 (Periodic B-spline)**.** Let $I = [0,1]$, $p \in \mathbb{N}$, $N \in \mathbb{N}_+$ with $N > p$, and $h = 1/N$. We define a *periodic B-spline basis function of degree p* $B_{p,i} = B_{h,p,i}$ by

$$B_{p,i} = \begin{cases} \text{equation (14)}, & \text{if } i = 1, 2, \dots, p, \\ N_{p,i}^{\Xi}|_I, & \text{if } i = p+1, p+2, \dots, N, \end{cases}$$

where Ξ is a knot vector defined by (13). We also define a *closed B-spline curve* as a curve $\mathbf{u}\colon I \to \mathbb{R}^2$ expressed by

$$\mathbf{u}(z) = \sum_{i=1}^{N} B_{p,i}(z)\mathbf{P}_i, \quad z \in I,$$

for some $\{\mathbf{P}_i\}_{i=1}^N \subset \mathbb{R}^2$. Finally, we define the space of closed B-spline curves by

$$\mathbf{B}_N^p := \left\{ \mathbf{u}(z) = \sum_{i=1}^{N} B_{p,i}(z)\mathbf{P}_i \;\middle|\; \mathbf{P}_i \in \mathbb{R}^2 \right\}.$$

We illustrate the figure of $B_{p,i}$ for $p = 3$ in Figure 1. One can observe that each $B_{p,i}$ has a compact support. Indeed, one can show that $\operatorname{supp} N_{p,i}^{\Xi} = [\xi_i, \xi_{i+p+1}]$ in general. Thus matrices appearing in the Galerkin method are sparse as in the usual FEM.

Since $\mathbf{B}_N^p \subset \mathbf{H}_\pi^2$ for $p \geq 2$, we can formulate the Galerkin approximation for (12).

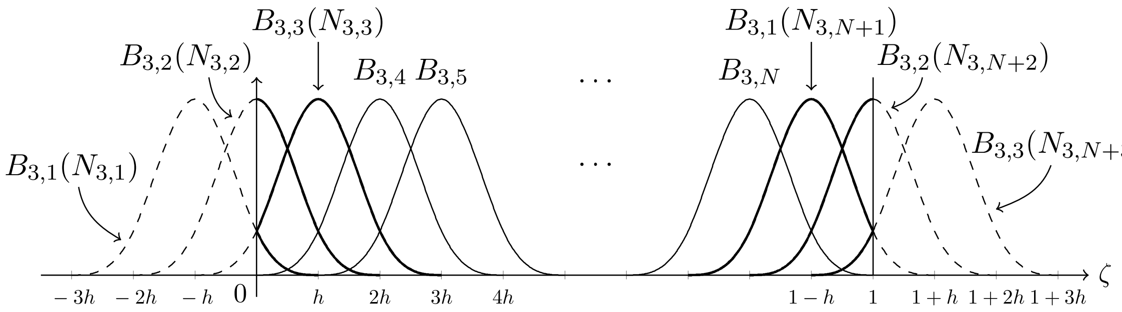

Figure 1: Periodic B-spline basis functions $B_{p,i}$ for $p = 3$ on I.

Scheme 1. Let $p \geq 2$. For given $\mathbf{u}_h^n \in \mathbf{B}_N^p$, find $\mathbf{u}_h^{n+1} \in \mathbf{B}_N^p$ that satisfies

$$\left(\left| \frac{\mathbf{u}_{h,z}^{n+1} + \mathbf{u}_{h,z}^n}{2} \right| \frac{\mathbf{u}_h^{n+1} - \mathbf{u}_h^n}{\tau_n}, \mathbf{v}_h \right)_I = -\left(\frac{\partial G_d}{\partial(\mathbf{u}_{h,z}^{n+1}, \mathbf{u}_{h,z}^n)}, \mathbf{v}_{h,z} \right)_I - \left(\frac{\partial G_d}{\partial(\mathbf{u}_{h,zz}^{n+1}, \mathbf{u}_{h,zz}^n)}, \mathbf{v}_{h,zz} \right)_I, \qquad \forall \mathbf{v}_h \in \mathbf{B}_N^p. \quad (15)$$

As mentioned in the previous section, we can show that the scheme preserves the energy dissipation.

Lemma 4.3. *Let $\{\mathbf{u}_h^n\}_n \subset \mathbf{B}_N^p$ be the solution of* (15)*. Then, for any $\tau_n > 0$ and $n \in \mathbb{N}_+$, we have $E[\mathbf{u}_h^{n+1}] \leq E[\mathbf{u}_h^n]$.*

Proof. Substituting $\mathbf{v}_h = (\mathbf{u}_h^{n+1} - \mathbf{u}_h^n)/\tau_n \in \mathbf{B}_N^p$ into (15), we have

$$\frac{E[\mathbf{u}_h^{n+1}] - E[\mathbf{u}_h^n]}{\tau_n} = -\int_0^1 \left| \frac{\mathbf{u}_h^{n+1} - \mathbf{u}_h^n}{\tau_n} \right|^2 \left| \frac{\mathbf{u}_{h,z}^{n+1} + \mathbf{u}_{h,z}^n}{2} \right| dz \leq 0,$$

which is the desired estimate. □

5. Examples of discrete gradient

In this section, we present the discrete gradients for the curve shortening flow (2) and the elastic flow (3) as examples. We first consider the curve shortening flow. Let $L[\mathbf{v}] = \int ds$ be the length functional for $\mathbf{v} \in \mathbf{H}_\pi^1$. Then, for $\mathbf{u}, \mathbf{v} \in \mathbf{H}_\pi^1$, we have

$$\begin{aligned} L[\mathbf{u}] - L[\mathbf{v}] &= \int_I (|\mathbf{u}_z| - |\mathbf{v}_z|)\, dz \\ &= \int_I \frac{\mathbf{u}_z + \mathbf{v}_z}{|\mathbf{u}_z| + |\mathbf{v}_z|} \cdot (\mathbf{u} - \mathbf{v})_z\, dz \\ &= -\int_I \frac{\partial}{\partial z} \left(\frac{\mathbf{u}_z + \mathbf{v}_z}{|\mathbf{u}_z| + |\mathbf{v}_z|} \right) \cdot (\mathbf{u} - \mathbf{v})\, dz \\ &= -\int \left| \frac{\mathbf{u}_z + \mathbf{v}_z}{2} \right|^{-1} \frac{\partial}{\partial z} \left(\frac{\mathbf{u}_z + \mathbf{v}_z}{|\mathbf{u}_z| + |\mathbf{v}_z|} \right) \cdot (\mathbf{u} - \mathbf{v})\, ds\left(\frac{\mathbf{u} + \mathbf{v}}{2} \right). \end{aligned}$$

Thus, in this case, we can define the discrete gradient by

$$\operatorname{grad}_{\mathrm{d}} L(\mathbf{u},\mathbf{v}) := -\left|\frac{\mathbf{u}_z+\mathbf{v}_z}{2}\right|^{-1}\frac{\partial}{\partial z}\left(\frac{\mathbf{u}_z+\mathbf{v}_z}{|\mathbf{u}_z|+|\mathbf{v}_z|}\right). \tag{16}$$

We next consider the elastic flow. Let $E[\mathbf{u}] = \int(\varepsilon^2|\boldsymbol{\kappa}|^2+1)ds$ be the elastic energy for $\mathbf{u}\in\mathbf{H}^2_\pi$. Furthermore, let $B[\mathbf{u}] = \int|\boldsymbol{\kappa}|^2 ds$ be the bending energy so that $E = \varepsilon^2 B + L$. We now derive $\operatorname{grad}_{\mathrm{d}} B$. We recall that the bending energy B can be written as

$$B[\mathbf{u}] = \int_0^1 \frac{\det(\mathbf{u}_z,\mathbf{u}_{zz})^2}{|\mathbf{u}_z|^5}dz, \quad \mathbf{u}\in\mathbf{H}^2_\pi,$$

where $\det(\mathbf{u},\mathbf{v}) = u_1v_2 - u_2v_1$. Therefore, it suffices to derive the discrete partial derivatives of the density functional

$$G(\mathbf{u}_z,\mathbf{u}_{zz}) = \frac{\det(\mathbf{u}_z,\mathbf{u}_{zz})^2}{|\mathbf{u}_z|^5}.$$

Let $\mathbf{u},\mathbf{v}\in\mathbf{H}^2_\pi$. Then, we have

$$\begin{aligned}G(\mathbf{u}_z,\mathbf{u}_{zz}) - G(\mathbf{v}_z,\mathbf{v}_{zz}) &= \left(\frac{1}{|\mathbf{u}_z|^5}-\frac{1}{|\mathbf{v}_z|^5}\right)\frac{\det(\mathbf{u}_z,\mathbf{u}_{zz})^2+\det(\mathbf{v}_z,\mathbf{v}_{zz})^2}{2}\\ &\quad+\frac{|\mathbf{u}_z|^{-5}+|\mathbf{v}_z|^{-5}}{2}\Big[\det(\mathbf{u}_z,\mathbf{u}_{zz})^2-\det(\mathbf{v}_z,\mathbf{v}_{zz})^2\Big]. \end{aligned}\tag{17}$$

The first term can be addressed by the following calculation:

$$\frac{1}{|\mathbf{u}_z|^5}-\frac{1}{|\mathbf{v}_z|^5} = -\frac{|\mathbf{u}_z|^5-|\mathbf{v}_z|^5}{|\mathbf{u}_z|^5|\mathbf{v}_z|^5} = -\frac{\sum_{j=0}^4|\mathbf{u}_z|^j|\mathbf{v}_z|^{4-j}}{|\mathbf{u}_z|^5|\mathbf{v}_z|^5(|\mathbf{u}_z|+|\mathbf{v}_z|)}(\mathbf{u}_z+\mathbf{v}_z)\cdot(\mathbf{u}_z-\mathbf{v}_z). \tag{18}$$

From the bilinearity of the determinant, we have

$$\det(\mathbf{u}_z,\mathbf{u}_{zz}) - \det(\mathbf{v}_z,\mathbf{v}_{zz}) = \det\left(\mathbf{u}_z-\mathbf{v}_z, \frac{\mathbf{u}_{zz}+\mathbf{v}_{zz}}{2}\right) + \det\left(\frac{\mathbf{u}_z+\mathbf{v}_z}{2}, \mathbf{u}_{zz}-\mathbf{v}_{zz}\right). \tag{19}$$

Summarizing (17), (18), and (19), we have

$$\begin{aligned}
\frac{\partial G_{\mathrm{d}}}{\partial(u_{1,z},v_{1,z})} &= -\frac{\sum_{j=0}^4|\mathbf{u}_z|^j|\mathbf{v}_z|^{4-j}}{|\mathbf{u}_z|^5|\mathbf{v}_z|^5(|\mathbf{u}_z|+|\mathbf{v}_z|)}\frac{\det(\mathbf{u}_z,\mathbf{u}_{zz})^2+\det(\mathbf{v}_z,\mathbf{v}_{zz})^2}{2}(u_{1,z}+v_{1,z})\\
&\quad+\frac{|\mathbf{u}_z|^{-5}+|\mathbf{v}_z|^{-5}}{2}[\det(\mathbf{u}_z,\mathbf{u}_{zz})+\det(\mathbf{v}_z,\mathbf{v}_{zz})]\frac{u_{2,zz}+v_{2,zz}}{2},\\
\frac{\partial G_{\mathrm{d}}}{\partial(u_{2,z},v_{2,z})} &= -\frac{\sum_{j=0}^4|\mathbf{u}_z|^j|\mathbf{v}_z|^{4-j}}{|\mathbf{u}_z|^5|\mathbf{v}_z|^5(|\mathbf{u}_z|+|\mathbf{v}_z|)}\frac{\det(\mathbf{u}_z,\mathbf{u}_{zz})^2+\det(\mathbf{v}_z,\mathbf{v}_{zz})^2}{2}(u_{2,z}+v_{2,z})\\
&\quad-\frac{|\mathbf{u}_z|^{-5}+|\mathbf{v}_z|^{-5}}{2}[\det(\mathbf{u}_z,\mathbf{u}_{zz})+\det(\mathbf{v}_z,\mathbf{v}_{zz})]\frac{u_{1,zz}+v_{1,zz}}{2},\\
\frac{\partial G_{\mathrm{d}}}{\partial(u_{1,zz},v_{1,zz})} &= -\frac{|\mathbf{u}_z|^{-5}+|\mathbf{v}_z|^{-5}}{2}[\det(\mathbf{u}_z,\mathbf{u}_{zz})+\det(\mathbf{v}_z,\mathbf{v}_{zz})]\frac{u_{2,z}+v_{2,z}}{2},
\end{aligned}$$

$$\frac{\partial G_{\mathrm{d}}}{\partial(u_{2,zz}, v_{2,zz})} = \frac{|\mathbf{u}_z|^{-5} + |\mathbf{v}_z|^{-5}}{2}[\det(\mathbf{u}_z, \mathbf{u}_{zz}) + \det(\mathbf{v}_z, \mathbf{v}_{zz})]\frac{u_{1,z} + v_{1,z}}{2}.$$

Hence we can compute $\operatorname{grad}_{\mathrm{d}} B(\mathbf{u}, \mathbf{v})$ by

$$\operatorname{grad}_{\mathrm{d}} B(\mathbf{u}, \mathbf{v}) = -\frac{\partial}{\partial z}\frac{\partial G_{\mathrm{d}}}{\partial(\mathbf{u}_z, \mathbf{v}_z)} + \frac{\partial^2}{\partial z^2}\frac{\partial G_{\mathrm{d}}}{\partial(\mathbf{u}_{zz}, \mathbf{v}_{zz})},$$

and eventually we obtain the discrete gradient for the elastic energy by

$$\operatorname{grad}_{\mathrm{d}} E(\mathbf{u}, \mathbf{v}) = \varepsilon^2 \operatorname{grad}_{\mathrm{d}} B(\mathbf{u}, \mathbf{v}) + \operatorname{grad}_{\mathrm{d}} L(\mathbf{u}, \mathbf{v}).$$

6. Area preserving curve shortening flow

In this section, we construct a novel structure-preserving scheme for area-preserving curve shortening flow (4). The purpose of this section is to derive the temporally discretized scheme for (4) in the weak formulation that satisfies the discrete energy dissipation $L[\mathbf{u}^{n+1}] \leq L[\mathbf{u}^n]$ and the area preservation $A[\mathbf{u}^{n+1}] = A[\mathbf{u}^n]$, where $A[\mathbf{u}]$ is the area of the domain enclosed by the curve $\mathbf{u}$ and written as

$$A[\mathbf{u}] = \frac{1}{2}\int \mathbf{u} \cdot \boldsymbol{\nu} ds$$

for $\mathbf{u} \in \mathbf{H}^1_\pi$. The result of this section was obtained *after* the conference.

We first review the derivation of the equation (4). Let $\lambda \in \mathbb{R}$ be the Lagrange multiplier and consider an auxiliary functional $E[\mathbf{u}] = L[\mathbf{u}] + \lambda A[\mathbf{u}]$. Then, since $\operatorname{grad} L(\mathbf{u}) = -\boldsymbol{\kappa}$ and $\operatorname{grad} A(\mathbf{u}) = \boldsymbol{\nu}$, the gradient flow for E is written as

$$\mathbf{u}_t = \boldsymbol{\kappa} - \lambda \boldsymbol{\nu}. \tag{20}$$

Multiplying this by $\boldsymbol{\nu}$ and integrating over the curve $\mathbf{u}$, we have

$$\frac{d}{dt}A[\mathbf{u}] = \int \boldsymbol{\kappa} \cdot \boldsymbol{\nu} ds - \lambda L[\mathbf{u}],$$

since the chain rule for A is described as

$$\frac{d}{dt}A[\mathbf{u}] = \int \boldsymbol{\nu} \cdot \mathbf{u}_t ds,$$

for an evolving curve $\mathbf{u}$. Hence, if we set $\lambda = L[\mathbf{u}]^{-1}\int \boldsymbol{\kappa} \cdot \boldsymbol{\nu} ds$, we obtain $\frac{d}{dt}A[\mathbf{u}] = 0$ and the gradient flow is given by (4). Furthermore, multiplying (20) by $\mathbf{u}_t$ and integrating over the curve $\mathbf{u}$, we have

$$\int |\mathbf{u}_t|^2 ds = -\frac{d}{dt}L[\mathbf{u}] - \lambda\frac{d}{dt}A[\mathbf{u}],$$

which implies $\frac{d}{dt}L[\mathbf{u}] \leq 0$ since the area is preserved.

Now, we discretize the above procedure. To do that, we set

$$\begin{pmatrix} a \\ b \end{pmatrix}^{\perp} := \begin{pmatrix} b \\ -a \end{pmatrix},$$

which is the rotated vector. Then, the outward unit normal vector of $\mathbf{u}$ is described by $\boldsymbol{\nu} = \boldsymbol{\nu}(\mathbf{u}) = \mathbf{u}_s^\perp$, where $\mathbf{u}_s$ is the arc-length derivative. Let $\mathbf{u}, \mathbf{v} \in \mathbf{H}^1_\pi$. Then, we have

$$\begin{aligned} A[\mathbf{u}] - A[\mathbf{v}] &= \frac{1}{2}\int_0^1 (\mathbf{u}\cdot\mathbf{u}_z^\perp - \mathbf{v}\cdot\mathbf{v}_z^\perp)dz \\ &= \frac{1}{2}\int_0^1 \left[(\mathbf{u}-\mathbf{v})\cdot\frac{\mathbf{u}_z^\perp + \mathbf{v}_z^\perp}{2} + \frac{\mathbf{u}+\mathbf{v}}{2}\cdot(\mathbf{u}_z^\perp - \mathbf{v}_z^\perp)\right]dz \\ &= \frac{1}{2}\int_0^1 \left[(\mathbf{u}-\mathbf{v})\cdot\frac{\mathbf{u}_z^\perp + \mathbf{v}_z^\perp}{2} - \frac{\mathbf{u}_z+\mathbf{v}_z}{2}\cdot(\mathbf{u}^\perp - \mathbf{v}^\perp)\right]dz \\ &= \int_0^1 (\mathbf{u}-\mathbf{v})\cdot\frac{\mathbf{u}_z^\perp + \mathbf{v}_z^\perp}{2}dz. \end{aligned}$$

Here, we used the fact that $\mathbf{u}\cdot\mathbf{v}^\perp = -\mathbf{u}^\perp\cdot\mathbf{v}$. Therefore, it is natural to define the discrete gradient of A by

$$\operatorname{grad}_{\mathrm{d}} A(\mathbf{u},\mathbf{v}) = \left|\frac{\mathbf{u}_z+\mathbf{v}_z}{2}\right|^{-1}\left(\frac{\mathbf{u}_z+\mathbf{v}_z}{2}\right)^\perp = \boldsymbol{\nu}\Big(\frac{\mathbf{u}+\mathbf{v}}{2}\Big).$$

With this notation, we obtain the following discrete chain rule for A:

$$A[\mathbf{u}] - A[\mathbf{v}] = \int \boldsymbol{\nu}\Big(\frac{\mathbf{u}+\mathbf{v}}{2}\Big)\cdot(\mathbf{u}-\mathbf{v})ds\Big(\frac{\mathbf{u}+\mathbf{v}}{2}\Big). \tag{21}$$

In the definition of the discrete gradient in Section 3, we mentioned that there may several choices of the line element. However, in view of the above calculation, it is natural to choose $ds((\mathbf{u}+\mathbf{v})/2)$.

Since the discrete gradient of the length functional L is given by (16), the discrete gradient flow for $E = L + \lambda A$ is described as

$$\frac{\mathbf{u}^{n+1}-\mathbf{u}^n}{\tau_n} = \left|\frac{\mathbf{u}_z^{n+1}+\mathbf{u}_z^n}{2}\right|^{-1}\frac{\partial}{\partial z}\left(\frac{\mathbf{u}_z^{n+1}+\mathbf{u}_z^n}{|\mathbf{u}_z^{n+1}|+|\mathbf{u}_z^n|}\right) - \lambda\boldsymbol{\nu}\left(\frac{\mathbf{u}^{n+1}+\mathbf{u}^n}{2}\right),$$

and the weak formulation is

$$\begin{aligned} &\left(\left|\frac{\mathbf{u}_z^{n+1}+\mathbf{u}_z^n}{2}\right|\frac{\mathbf{u}^{n+1}-\mathbf{u}^n}{\tau_n}, \mathbf{v}\right)_I \\ &= -\left(\frac{\mathbf{u}_z^{n+1}+\mathbf{u}_z^n}{|\mathbf{u}_z^{n+1}|+|\mathbf{u}_z^n|}, \mathbf{v}_z\right)_I - \lambda\left(\left|\frac{\mathbf{u}_z^{n+1}+\mathbf{u}_z^n}{2}\right|\boldsymbol{\nu}\left(\frac{\mathbf{u}^{n+1}+\mathbf{u}^n}{2}\right), \mathbf{v}\right)_I, \qquad \forall\mathbf{v}\in\mathbf{H}^1_\pi. \end{aligned} \tag{22}$$

In the continuous case, we multiplied the gradient flow by the normal vector $\boldsymbol{\nu}$ to determine the Lagrange multiplier. Therefore, we want to substitute $\mathbf{v} = \boldsymbol{\nu}$ in the weak formulation; nevertheless, $\boldsymbol{\nu}(\mathbf{u}) \notin \mathbf{H}^1_\pi$ if $\mathbf{u} \in \mathbf{H}^1_\pi$. To overcome this issue, we introduce the projection of the normal velocity. In view of the Galerkin approximation, we consider the projection onto a subspace of $\mathbf{H}^1_\pi$.

Definition 6.1. Let $\mathbf{V} \subset \mathbf{H}^1_\pi$ be a subspace and $\mathbf{u} \in \mathbf{H}^1_\pi$. Then, we define the projection operator $P_{V,\mathbf{u}}\colon L^2(I)^2 \to \mathbf{V}$ by

$$\int_0^1 (P_{V,\mathbf{u}}\mathbf{w})\cdot\mathbf{v}|\mathbf{u}_z|dz = \int_0^1 \mathbf{w}\cdot\mathbf{v}|\mathbf{u}_z|dz, \qquad \forall\mathbf{v}\in\mathbf{V},$$

for $\mathbf{w} \in L^2(I)^2$.

Now, let $\mathbf{u}^{n+1/2} := (\mathbf{u}^{n+1} + \mathbf{u}^n)/2$ and $\tilde{\boldsymbol{\nu}} := P_{\mathbf{H}^1_\pi, \mathbf{u}^{n+1/2}} \boldsymbol{\nu}(\mathbf{u}^{n+1/2})$. We set $\mathbf{v} = \tilde{\boldsymbol{\nu}}$ in (22). Then, the left-hand-side becomes

$$\begin{aligned} \left(\left| \frac{\mathbf{u}_z^{n+1} + \mathbf{u}_z^n}{2} \right| \frac{\mathbf{u}^{n+1} - \mathbf{u}^n}{\tau_n}, \tilde{\boldsymbol{\nu}} \right)_I &= \int \boldsymbol{\nu}(\mathbf{u}^{n+1/2}) \cdot \frac{\mathbf{u}^{n+1} - \mathbf{u}^n}{\tau_n} ds(\mathbf{u}^{n+1/2}) \\ &= \frac{A[\mathbf{u}^{n+1}] - A[\mathbf{u}^n]}{\tau_n} \end{aligned}$$

by the definition of $\tilde{\boldsymbol{\nu}}$ and the discrete chain rule (21). Further, the right-hand-side of (22) becomes

$$-\int_0^1 \frac{\mathbf{u}_z^{n+1} + \mathbf{u}_z^n}{|\mathbf{u}_z^{n+1}| + |\mathbf{u}_z^n|} \cdot \tilde{\boldsymbol{\nu}}_z dz - \lambda \int |\tilde{\boldsymbol{\nu}}|^2 ds(\mathbf{u}^{n+1/2})$$

by the definition of $\tilde{\boldsymbol{\nu}}$. Hence, if we set

$$\lambda := -\left[\int |\tilde{\boldsymbol{\nu}}|^2 ds(\mathbf{u}^{n+1/2}) \right]^{-1} \int_0^1 \frac{\mathbf{u}_z^{n+1} + \mathbf{u}_z^n}{|\mathbf{u}_z^{n+1}| + |\mathbf{u}_z^n|} \cdot \tilde{\boldsymbol{\nu}}_z dz, \tag{23}$$

then, we can derive $A[\mathbf{u}^{n+1}] = A[\mathbf{u}^n]$, which is the discrete area preservation. Moreover, letting $\mathbf{v} = (\mathbf{u}^{n+1} - \mathbf{u}^n)/\tau_n$ in (22), we have

$$\int \left| \frac{\mathbf{u}^{n+1} - \mathbf{u}^n}{\tau_n} \right|^2 ds(\mathbf{u}^{n+1/2}) = -\frac{L[\mathbf{u}^{n+1}] - L[\mathbf{u}^n]}{\tau_n} - \lambda \frac{A[\mathbf{u}^{n+1}] - A[\mathbf{u}^n]}{\tau_n}$$

from the discrete chain rules. Therefore, the discrete area preservation property yields the discrete energy dissipation $L[\mathbf{u}^{n+1}] \le L[\mathbf{u}^n]$. Hence, the scheme (22) with the Lagrange multiplier λ given by (23) preserves both the area preservation and the energy dissipation. We here remark that the last term of (22) can be written as

$$\left(\left| \frac{\mathbf{u}_z^{n+1} + \mathbf{u}_z^n}{2} \right| \boldsymbol{\nu}\left(\frac{\mathbf{u}^{n+1} + \mathbf{u}^n}{2} \right), \mathbf{v} \right)_I = \left(|\mathbf{u}^{n+1/2}| \tilde{\boldsymbol{\nu}}, \mathbf{v} \right)_I$$

by the definition of $\tilde{\boldsymbol{\nu}}$.

The above argument is valid in the case of the Galerkin method. Thus we can derive the following fully discretized scheme for the area preserving curve shortening flow (4).

Scheme 2. For given $\mathbf{u}_h^n \in \mathbf{B}_N^p$, find $\mathbf{u}_h^{n+1} \in \mathbf{B}_N^p$ that satisfies

$$\begin{aligned} &\left(|\mathbf{u}_{h,z}^{n+1/2}| \frac{\mathbf{u}_h^{n+1} - \mathbf{u}_h^n}{\tau_n}, \mathbf{v}_h \right)_I \\ &\qquad = -\left(\frac{\mathbf{u}_{h,z}^{n+1} + \mathbf{u}_{h,z}^n}{|\mathbf{u}_{h,z}^{n+1}| + |\mathbf{u}_{h,z}^n|}, \mathbf{v}_{h,z} \right)_I - \lambda \left(|\mathbf{u}_{h,z}^{n+1/2}| \tilde{\boldsymbol{\nu}}_h, \mathbf{v}_h \right)_I, \qquad \forall \mathbf{v}_h \in \mathbf{B}_N^p, \end{aligned} \tag{24}$$

where $\mathbf{u}_h^{n+1/2} = (\mathbf{u}_h^{n+1} + \mathbf{u}_h^n)/2$, $\tilde{\boldsymbol{\nu}}_h \in \mathbf{B}_N^p$ is defined by

$$\int_0^1 \tilde{\boldsymbol{\nu}}_h \cdot \mathbf{v}_h |\mathbf{u}_{h,z}^{n+1/2}| dz = \int_0^1 \boldsymbol{\nu}(\mathbf{u}^{n+1/2}) \cdot \mathbf{v}_h |\mathbf{u}_{h,z}^{n+1/2}| dz, \qquad \forall \mathbf{v}_h \in \mathbf{B}_N^p,$$

and $\lambda \in \mathbb{R}$ is given by

$$\lambda = -\left[\int |\tilde{\boldsymbol{\nu}}_h|^2 ds(\mathbf{u}_h^{n+1/2}) \right]^{-1} \int_0^1 \frac{\mathbf{u}_{h,z}^{n+1} + \mathbf{u}_{h,z}^n}{|\mathbf{u}_{h,z}^{n+1}| + |\mathbf{u}_{h,z}^n|} \cdot \tilde{\boldsymbol{\nu}}_{h,z} dz.$$

By the same argument as in the semi-discrete case, we can show that the scheme preserves both the area preservation and the energy dissipation.

Lemma 6.2. *Let $\{\mathbf{u}_h^n\}_n \subset \mathbf{B}_N^p$ be the solution of* (24)*. Then, for any $\tau_n > 0$ and $n \in \mathbb{N}_+$, we have $A[\mathbf{u}_h^{n+1}] = A[\mathbf{u}_h^n]$ and $L[\mathbf{u}_h^{n+1}] \leq L[\mathbf{u}_h^n]$.*

7. Numerical examples

In this section, we present several numerical examples. We will test our schemes (15) and (24) and observe that energy dissipation and the area preservation are preserved. Examples of the first scheme are the same as those given in [5].

7.1. Elastic flow

We present some numerical examples of the elastic flow (3) with a small parameter ε computed by our scheme (15). The corresponding functional and its discrete gradient are presented in Section 5. It is known that equation (3) has a unique time-global solution (see, e.g., [1, Theorem 3.2]). Therefore, the turning number $|\int \boldsymbol{\kappa} ds|/(2\pi) \in \mathbb{N}$ is invariant.

In the following examples, we developed several techniques for stable computation. For example, we choose appropriate time increment τ_n according to the speed of energy dissipation. We refer the reader to [5] for precise techniques of numerical experiments. Videos illustrating the following examples are available on YouTube[1].

Before presenting numerical examples, we recall the steady-state solutions for the elastic flow. It is known that steady closed curves of the elastic energy are the circle of radius ε, the figure-eight-shaped curve with scale ε, and their multiple versions (see Figure 2 and [6, 12]). Their energies are

$$E[\text{circle}] = 4\pi\varepsilon, \quad E[\text{eight-shaped}] \approx \varepsilon \cdot 21.2075,$$

respectively. The exact value of the latter energy is expressed by the elliptic integrals (cf. [10]).

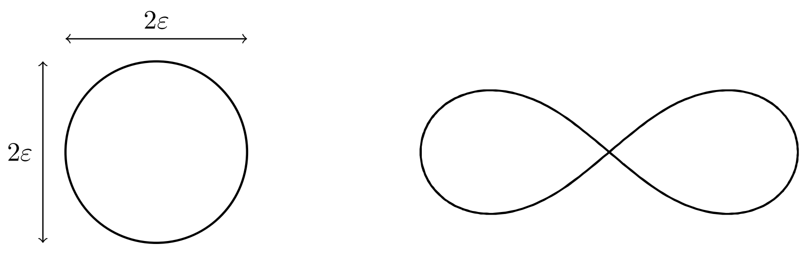

Figure 2: Steady states of the elastic energy.

Example 7.1. We first show the simplest example with a circular initial curve. In this case, the exact solution is a circle at every time, and the steady state is the circle of radius

[1]URL: `https://www.youtube.com/playlist?list=PLMF3dSqWEii69loXvCtgDCI4PYijq_4L3`

ε as mentioned above. Figure 3(a) shows the evolution of the curve at $t \approx 0, 0.1, \dots, 0.6$, with parameters

$$p = 3, \quad \varepsilon = 0.1, \quad N = 6, \quad \tau_n = 0.01,$$

where the initial curve is the L^2-projection of the unit circle. We can observe that six control points are sufficient to express a circle by a B-spline curve. The energy at $t \approx 0.6$ is $E \approx 1.2583$, which approximates the exact value of the energy at the steady state $4\pi\varepsilon \approx 1.2566$. Figure 3(b) shows the evolution of the energy. The discrete energy dissipation property is clearly visible. In Figure 3(a), one can observe that the curve shrinks like the curvature flow (2) until $t \approx 0.5$, and it stops shrinking when the radius approaches to ε.

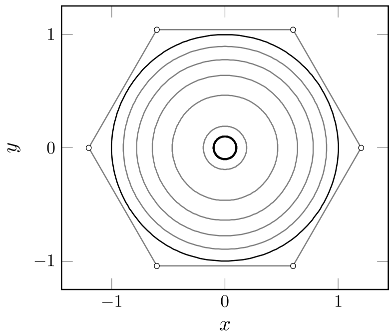

(a) Evolution of the circle. The outermost curve and the innermost one are at times $t = 0$, and $t \approx 0.6$, respectively.

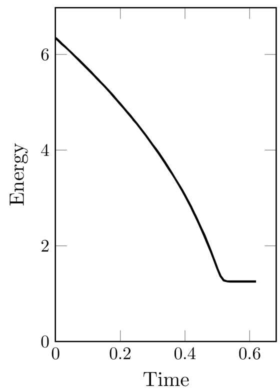

(b) Evolution of the energy.

Figure 3: Example 7.1.

Example 7.2. The second example is shown in Figure 4. The initial curve is figure-eight-shaped. The parameters are

$$p = 3, \quad \varepsilon = 0.2, \quad N = 12, \quad \tau_n \leq 0.01.$$

Figure 4(a) shows the evolution of the curve at $t \approx 0, 0.2, \dots, 1.2$ and Figure 4(b) shows the evolution of the energy. The energy at $t \approx 1.2$ is $E \approx 4.2433$, which approximates the exact value of the energy at the steady state ≈ 4.2415.

In Figure 4(a), initially the small loop (the right loop) shrinks faster than the larger one. When the scale of the right loop becomes ε, the loop stops shrinking, and the left one begins to shrink. Finally, the left one also stops shrinking, and the curve approaches the steady state.

Example 7.3. The third example is shown in Figure 5. The initial shape of the curve is a cardioid-like curve as shown in Figure 5(a). The parameters of the curve are

$$p = 3, \quad \varepsilon = 0.1, \quad N = 12, \quad \tau \leq 0.005.$$

Figure 5 shows the evolution of the curve at $t \approx 0, 0.2, 0.4, 0.6$ and Figure 6 shows the evolution of the energy. In this case, the steady state is a double-looped circle with radius $\varepsilon = 0.1$. Therefore, the energy of the solution at $t \approx 0.6$ ($E \approx 2.5228$) is approximately twice the value of that of Example 7.1.

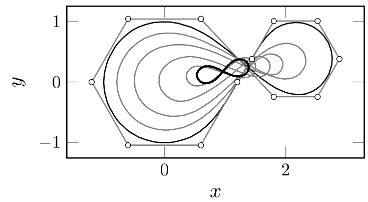

(a) Evolution of the figure-eight-shaped curve. The outermost curve is the initial shape of the curve, and the innermost one is the curve at $t \approx 1.2$.

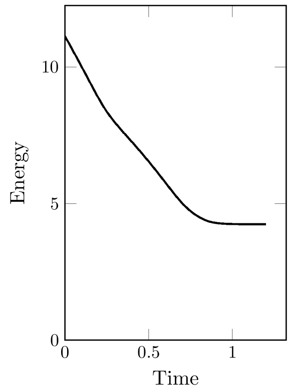

(b) Evolution of the energy.

Figure 4: Example 7.2.

The behavior of the curve is similar to Example 7.2. That is, initially the smaller loop shrinks until the scale is approximately ε. Then, the larger one shrinks and the curve approaches the steady state.

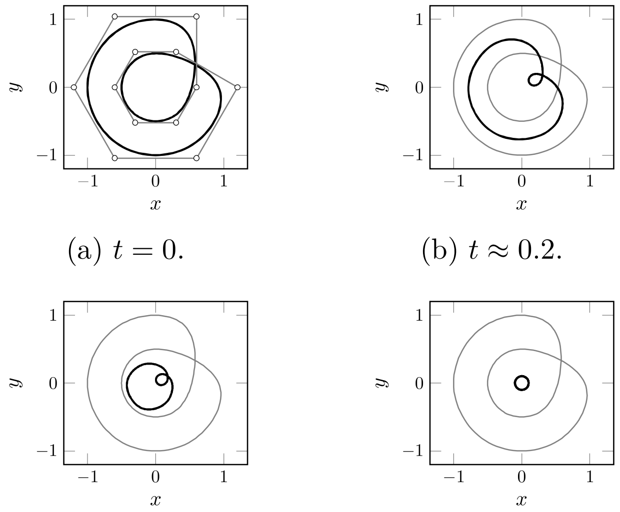

(a) $t = 0$.

(b) $t \approx 0.2$.

(c) $t \approx 0.4$.

(d) $t \approx 0.6$.

Figure 5: Evolution of the curves of Example 7.3.

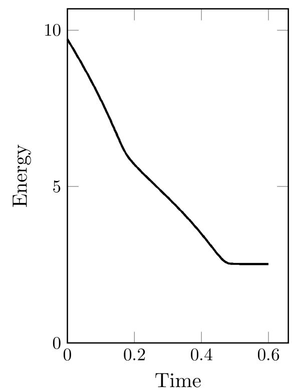

Figure 6: Evolution of the energy of Example 7.3.

Example 7.4. This example shows a topology-changing solution. The initial curve is shown in Figure 7(a), and Figure 7 shows its evolution. Figures 8 illustrates the evolution of the energy. The parameters are

$$p = 3, \quad \varepsilon = 0.2, \quad N \leq 20, \quad \tau_n \leq 0.005.$$

One can observe that the topology of the curve changes at around $t = 1.05$ (Figures 7(d) and (e)). At the same time, the energy decreases drastically (Figure 8).

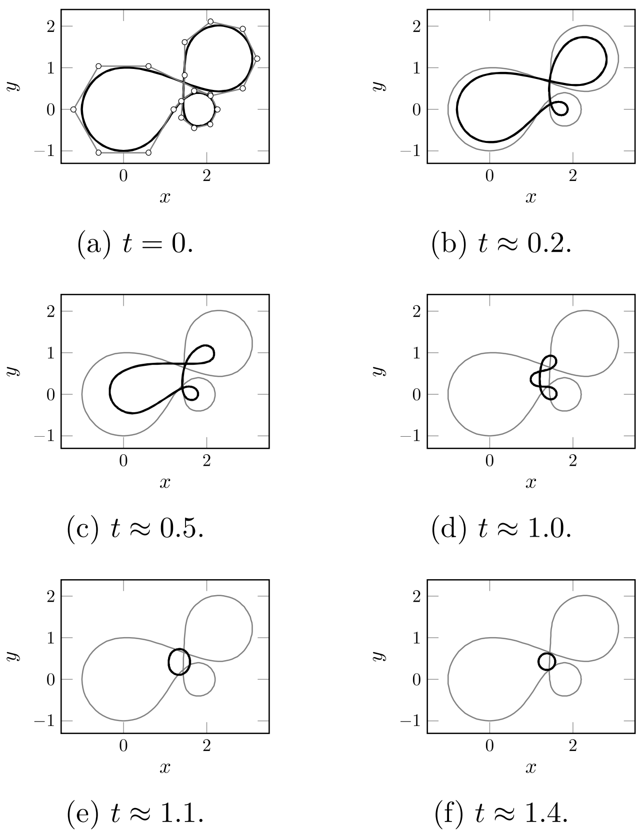

Figure 7: Evolution of the curves of Example 7.4.

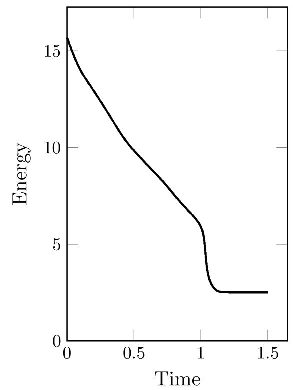

Figure 8: Evolution of the energy of Example 7.4.

Example 7.5. The following two examples investigate problems with more complicated solutions. The initial shape of the curve is shown in Figure 9(a), and Figure 9 shows its evolution. Figures 10 illustrates the evolution of the energy. The parameters are

$$p = 3, \quad \varepsilon = 0.2, \quad N \leq 49, \quad \tau_n \leq 0.005.$$

In this example, the topology of the curve changes frequently. For example, the loop in the upper left of the curve disappears at around $t = 1.35$. Since the turning number of the initial curve is zero, we can easily determine before computation that the steady state is a figure-eight-shaped curve. However, the evolution of the curve is quite complicated so that we cannot predict the behavior. When the topology changes, the energy decreases rapidly as in Example 7.4.

Example 7.6. The initial curve for this example is shown in Figure 11(a), and Figure 11 shows its evolution. Figure 12 illustrates the evolution of the energy. The parameters are

$$p = 3, \quad \varepsilon = 0.2, \quad N \leq 54, \quad \tau_n \leq 0.005.$$

The solution displays complicated behavior as in Example 7.5, and the topology changes frequently. Since the turning number of the initial curve is one, the steady state is a circle with radius ε. However, as in the previous example, the evolution is too complicated to predict. One can observe that the energy decreases drastically when the topology changes as in the previous examples.

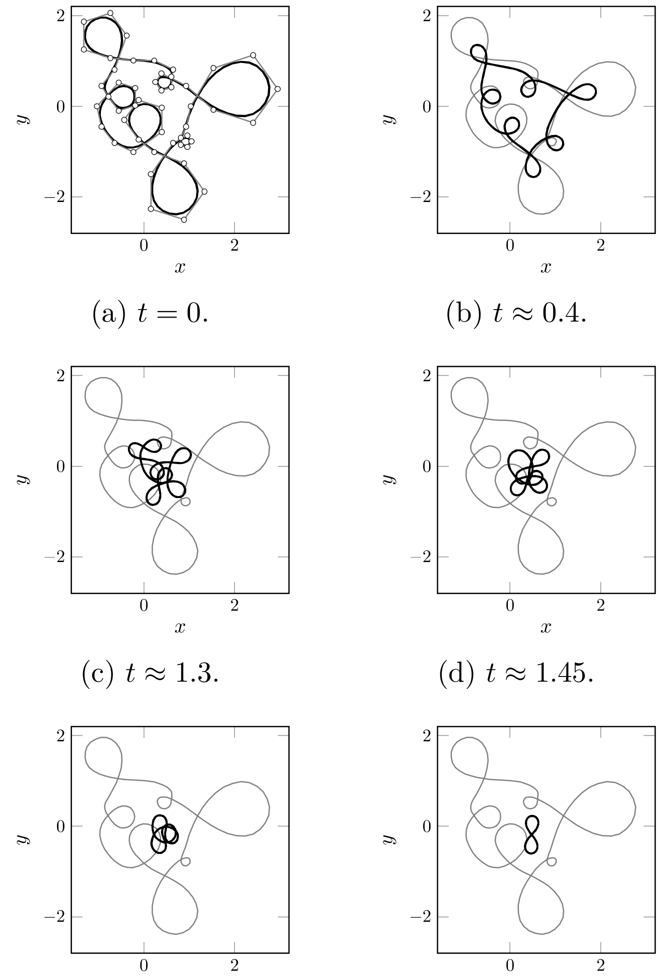

(a) $t = 0$.

(b) $t \approx 0.4$.

(c) $t \approx 1.3$.

(d) $t \approx 1.45$.

(e) $t \approx 1.65$.

(f) $t \approx 2.0$.

Figure 9: Evolution of the curves of Example 7.5.

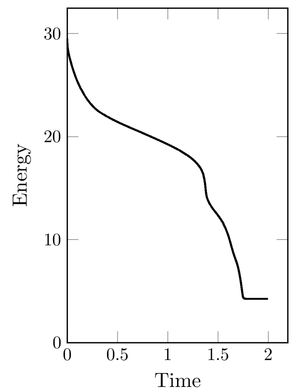

Figure 10: Evolution of the energy of Example 7.5.

7.2. Area preserving curve shortening flow

In this section, we present a numerical example of the area preserving curve shortening flow, which is computed by our scheme (24).

Example 7.7. The initial curve for this example is shown in Figure 13(a), and Figure 13 shows its evolution. Figures 14(a) and (b) illustrate the evolution of the length and the area, respectively. The parameters are

$$p = 3, \quad N = 21, \quad \tau_n = 0.01.$$

One can observe that the curve becomes convex and then goes to a circle. We can also observe that the length decreases monotonically. Moreover, we can conclude that the area is preserved since the scale of the vertical axis of Figure 14(b) is 10^{-9}.

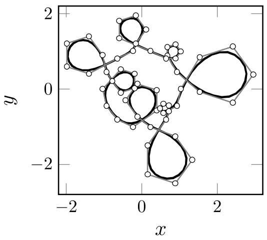

(a) $t = 0$.

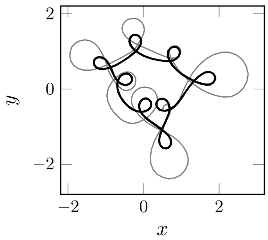

(b) $t \approx 0.4$.

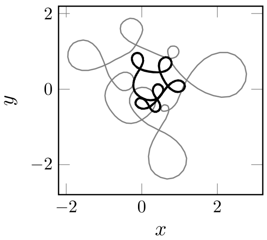

(c) $t \approx 1.3$.

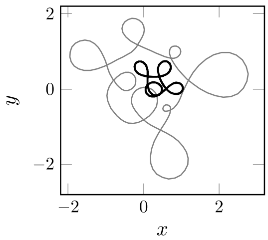

(d) $t \approx 1.5$.

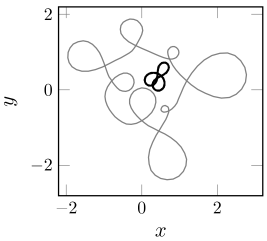

(e) $t \approx 1.9$.

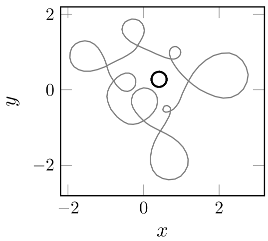

(f) $t \approx 2.3$.

Figure 11: Evolution of the curves of Example 7.6.

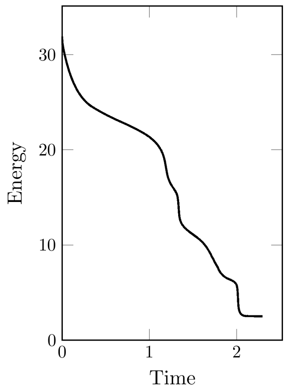

Figure 12: Evolution of the energy of Example 7.6.

8. Concluding remarks

In this study, we developed numerical schemes for gradient flows of planar curves that preserves the energy dissipation. The key-point is to discretize the chain rule for the energy functional, and this idea gives temporal discretization of the gradient flows. Moreover, with the aid of the smoothness of B-spline curves, we can construct fully discrete scheme without approximating curvatures.

We can also consider area preserving curve shortening flow, which is our ongoing work. We constructed numerical scheme that preserves both length dissipation and area preservation. Our idea is to discretize the chain rule and the Lagrange multiplier. Thus, it is expected that we can also construct a numerical scheme for Helfrich flow, which is the gradient flow for the bending energy $\int |\boldsymbol{\kappa} - \kappa_0 \mathbf{v}|^2 ds$ for a given constant κ_0 and has constraints that length and area are preserved.

Our scheme, however, only consider the normal direction of curves in a sense. Due to this, there are several examples that two control points becomes so close that the computation may break. In the theory of polygonal approximation of evolving curves, it is known that appropriate tangential velocity makes numerical computation stable. Thus, it may be interesting to investigate whether we can consider tangential velocity

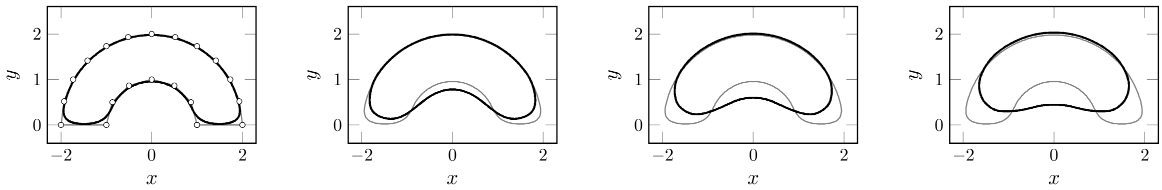

(a) $t = 0.0$. (b) $t = 0.1$. (c) $t = 0.2$. (d) $t = 0.3$.

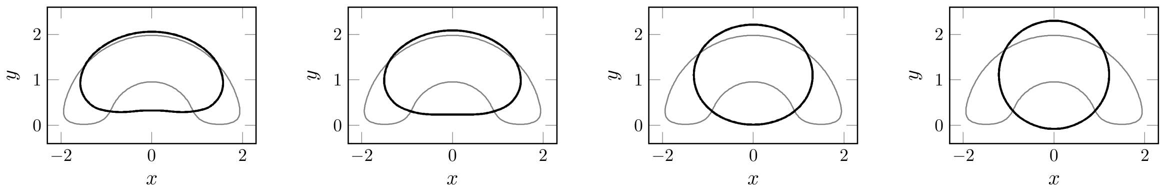

(e) $t = 0.4$. (f) $t = 0.5$. (g) $t = 1.0$. (h) $t = 2.0$.

Figure 13: Evolution of the curves of Example 7.7.

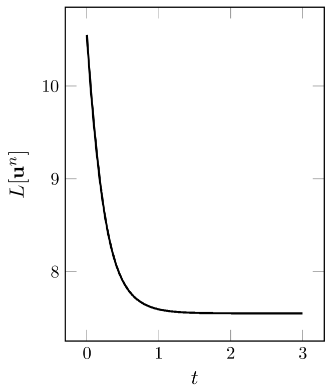

(a) Evolution of $L[\mathbf{u}^n]$.

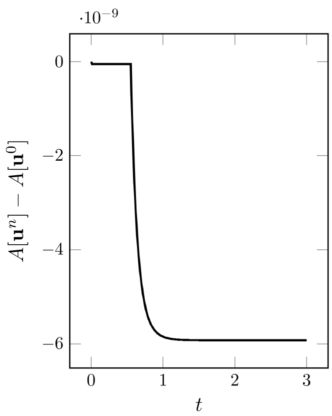

(b) Evolution of $A[\mathbf{u}^n] - A[\mathbf{u}^0]$.

Figure 14: Evolution of the length and area of Example 7.7.

that preserves the structure of flows. These problems remain an area for future work.

Acknowledgments

I would like to thank the organizers of the conference for giving me an opportunity to present our results and for their hospitality during the conference. Further, I would like to thank the Research Institute for Mathematical Sciences, Kyoto University for the financial support.

References

[1] G. Dziuk, E. Kuwert, and R. Schätzle. Evolution of elastic curves in $\mathbb{R}^n$: existence and computation. *SIAM J. Math. Anal.*, 33(5):1228–1245, 2002.

[2] G. E. Farin. *NURBS. From projective geometry to practical use.* A K Peters, Ltd., Natick, MA, second edition, 1999.

[3] D. Furihata and T. Matsuo. *Discrete variational derivative method. A structure-preserving numerical method for partial differential equations.* CRC Press, Boca Raton, FL, 2011.

[4] E. Hairer, C. Lubich, and G. Wanner. *Geometric numerical integration. Structure-preserving algorithms for ordinary differential equations.* Springer-Verlag, Berlin, second edition, 2006.

[5] T. Kemmochi. Energy dissipative numerical schemes for gradient flows of planar curves. *BIT*, 57(4):991–1017, 2017.

[6] A. E. H. Love. *A treatise on the Mathematical Theory of Elasticity.* Dover Publications, New York, 1944. Fourth Ed.

[7] T. Matsuo. Dissipative/conservative Galerkin method using discrete partial derivatives for nonlinear evolution equations. *J. Comput. Appl. Math.*, 218(2):506–521, 2008.

[8] M. Okumura. A stable and structure-preserving scheme for a non-local allenâĂŞcahn equation. *Japan J. Indust. Appl. Math.*, 35(3):1245–1281, 2018.

[9] L. Piegl and W. Tiller. *The NURBS book.* Springer, Berlin, second edition, 1997.

[10] Y. L. Sachkov. Closed Euler elasticae. *Tr. Mat. Inst. Steklova*, 278(Differentsialnye Uravneniya i Dinamicheskie Sistemy):227–241, 2012.

[11] L. L. Schumaker. *Spline functions: basic theory.* Cambridge University Press, Cambridge, third edition, 2007.

[12] D. A. Singer. Lectures on elastic curves and rods. In *Curvature and variational modeling in physics and biophysics*, volume 1002 of *AIP Conf. Proc.*, pages 3–32. Amer. Inst. Phys., Melville, NY, 2008.

Tomoya Kemmochi
Department of Applied Physics, Graduate School of Engineering, Nagoya University
Furo-cho, Chikusa-ku, Nagoya, Aichi, 464-8603, Japan
E-mail: `kemmochi@na.nuap.nagoya-u.ac.jp`
URL: `https://t-kemmochi.github.io`